

The one-loop tadpole in the geoSMEFT

T. Corbett¹,

¹ Niels Bohr International Academy,
 Niels Bohr Institute, University of Copenhagen,
 Blegdamsvej 17, DK-2100, Copenhagen, Denmark
 * corbett.t.s@gmail.com

August 16, 2021

1 Abstract

Making use of the geometric formulation of the Standard Model Effective Field Theory we calculate the one-loop tadpole diagrams to all orders in the Standard Model Effective Field Theory power counting. This work represents the first calculation of a one-loop amplitude beyond leading order in the Standard Model Effective Field Theory, and discusses the potential to extend this methodology to perform similar calculations of observables in the near future.

8

9 Contents

10	1 Introduction	1
11	2 Conventions	3
12	3 The all-orders vertices	6
13	4 Gauge fixing the geoSMEFT	9
14	5 The all-orders SMEFT tadpole	10
15	6 Conclusions	13
16	A Useful geoSMEFT definitions and relations	15
17	B Relevance of the tadpole to renormalization	16
18	References	17

19

20

21 1 Introduction

The Standard Model Effective Field Theory (SMEFT) has become a cornerstone of LHC searches for physics beyond the Standard Model (SM). The approach of the SMEFT is to search for the effects of non-resonant heavy new physics, which decouples as $1/\Lambda$, on measurable processes of the known particles. This approach makes two primary assumptions,

26 that the new physics is too heavy to directly produce at a collider and that the Higgs
 27 boson belongs to an $SU(2)_L$ doublet, as in the SM. With these assumptions the SMEFT
 28 is formulated as a tower of higher-dimensional operators suppressed by the new physics
 29 scale Λ and added to the SM Lagrangian:

$$\mathcal{L}_{\text{SMEFT}} = \mathcal{L}_{\text{SM}} + \sum_{n=5}^{\infty} \sum_i \frac{c_i}{\Lambda^{n-4}} \mathcal{O}_i. \quad (1)$$

30 Each subsequent power of $1/\Lambda$ should therefore be suppressed relative to the last, as Λ is
 31 a large mass scale well above that of a given scattering process.

32 For most LHC relevant processes the leading terms come from dimension-six operators
 33 suppressed by Λ^2 . There is ongoing discussion on how to handle the truncation of this
 34 series in the literature, i.e. to understand the error associated with truncating the series at
 35 a given order. Many groups have included squares of dimension-six operator contributions
 36 to amplitudes in their work, this allows for an inferred error by comparing results with
 37 and without the the dimension-six squared term. This presents a theoretical concern –
 38 formally this is not the full contribution at order $1/\Lambda^4$ as it neglects dimension-six squared
 39 contributions to the amplitude as well as dimension-eight operator effects. There is also
 40 the more practical issue, that in many instances the squared term results in more stringent
 41 constraints, a result of, for example, chiral suppression of the interference of the $1/\Lambda^2$ term
 42 with the SM. This makes a definition of truncation error in this way less than satisfactory.

43 An alternative approach is to compute the full contribution up to and including $\frac{1}{\Lambda^4}$
 44 effects. This suffers from the seemingly insurmountable number of parameters in the
 45 SMEFT beyond leading order. This is to a great degree controlled by only considering
 46 resonant processes where four-fermion operators can be neglected as well as making sim-
 47 plifying assumptions on the flavor structure of the SMEFT. To date three works have
 48 considered the full $\frac{1}{\Lambda^4}$ dependence in phenomenological studies. In [1], the authors study
 49 associated production of a Higgs boson with a W by meticulously elaborating all operators
 50 contributing via the Hilbert series method [2–4], and then performing a phenomenological
 51 study. Using a similar procedure the authors of [5] study the Drell Yan process at the
 52 LHC. In [6], the authors studied Z -pole observables and instead used the geometric for-
 53 mulation of the SMEFT which allows for, currently in limited cases, all orders calculations
 54 in the SMEFT power counting (i.e. the $1/\Lambda$ power counting).

55 The geometric SMEFT, or geoSMEFT, was born of an attempt to simplify the one loop
 56 calculation of $H \rightarrow \gamma\gamma$ [7, 8] and the resulting background gauge fixing of the SMEFT [9].
 57 Within this context it was realized that the SMEFT could be formulated in terms of
 58 *field-space connection matrices* of the form:

$$M_{I_1 \dots I_n} \sim \frac{\delta^n \mathcal{L}_{\text{SMEFT}}}{\delta \phi_{I_1} \dots \delta \phi_{I_n}} \Big|_{\mathcal{L}(\alpha, \beta, \dots) \rightarrow 0}. \quad (2)$$

59 These field-space connections are then matrices of products of the Higgs doublet with
 60 generators of $SU(2)_L$, and the evaluation at $\mathcal{L}(\alpha, \beta, \dots) \rightarrow 0$ represents setting various
 61 products of fields and their derivatives to zero. By constructing all gauge-variant, but
 62 Lorentz invariant, products of up to any three of the field strengths, covariant derivatives
 63 of the scalar field, and products of fermions, the geoSMEFT was formulated to include all
 64 three-point functions of SM fields plus arbitrarily many products of scalar fields [10]. This
 65 allowed for all-orders (in the SMEFT power counting) tree-level studies of the SMEFT
 66 in [11]. With all three-point functions defined to all orders in the geoSMEFT we can now
 67 use an alternative approach to studying the truncation error in the SMEFT. In [6] the
 68 full set of Z -pole observables at LEP were studied, and an alternative truncation error

69 estimate was proposed - varying the dependence on Wilson coefficients of the $1/\Lambda^4$ result
 70 in order to infer the error in the strictly $1/\Lambda^2$ terms.

71 With an enormous interest being generated around loop calculations in the SMEFT
 72 an important next obstacle for the geoSMEFT is to define a similar system for estimating
 73 truncation error at one loop. As mentioned above the geoSMEFT only includes vertices of
 74 three fields with an arbitrary number of scalar insertions. As such, the geoSMEFT is only
 75 suitable for the calculation of the tadpole diagram. This article demonstrates the ability
 76 to calculate the tadpole at one-loop and all orders in the SMEFT power counting and
 77 motivates further development of the geoSMEFT in order to allow consistently defined
 78 truncation errors at both tree- and one-loop level.

79 The article is organized as follows: In Section 2 we define the conventions used in
 80 the paper as well as introduce the set of relevant operator forms which contribute to
 81 the one-loop tadpole diagram, while in Section 3 we outline the Feynman rules derived
 82 from the classical Lagrangian. In Section 4 we gauge fix the geoSMEFT and derive the
 83 Feynman rules related to gauge fixing as well as the Feynman rules for ghosts. Then
 84 in Section 5 we give the main result of this article, the all orders tadpole, and Sec. 6 is
 85 dedicated to discussion of the outlook for the one-loop geoSMEFT and conclusions. The
 86 Appendix A includes relevant definitions and relations from the geoSMEFT which are
 87 used throughout this article, while App. B demonstrates the importance of the Tadpole
 88 diagram both phenomenologically and in preserving the gauge symmetry of the theory
 89 beyond tree level.

90 2 Conventions

91 In order to define the relevant terms of the Lagrangian for the calculation of the tadpole
 92 diagram, we follow the formulation of the geoSMEFT given in [10], as well as the gauge
 93 fixing of [9] and [12]. We begin by defining the field content of the geoSMEFT, the Higgs
 94 doublet of the the SM is rewritten in terms of a four-component real scalar field, ϕ^I by
 95 the following association:

$$H(\phi_I) = \frac{1}{\sqrt{2}} \begin{bmatrix} \phi_2 + i\phi_1 \\ \phi_4 - i\phi_3 \end{bmatrix}. \quad (3)$$

96 The $SU(2)_L$ and $U(1)_Y$ gauge bosons, B and W^I , are replaced with four component vector
 97 field $W^A = \{W^1, W^2, W^3, B\}$. These weak-eigenstate fields are transformed to the mass
 98 basis by the matrices:

$$\mathcal{U}_C^A \equiv \sqrt{g}^{AB} U_{BC}, \quad \mathcal{V}_K^I \equiv \sqrt{h}^{IJ} V_{JK}. \quad (4)$$

99 Above and in what follows latin indices are four-component unless otherwise specified.
 100 The matrices, \sqrt{g} and \sqrt{h} are defined below and are the inverse-square roots of the field-
 101 space connections of the field combinations $W_{\mu\nu}^A W^{B,\mu\nu}$ and $(D_\mu\phi)^I (D^\mu\phi)^J$ respectively.
 102 The matrices U and V take the weak eigenstate fields and rotate them to the physical
 103 basis of the SM, they are given by:

$$U_{BC} = \begin{bmatrix} \frac{1}{\sqrt{2}} & \frac{1}{\sqrt{2}} & 0 & 0 \\ \frac{i}{\sqrt{2}} & \frac{-i}{\sqrt{2}} & 0 & 0 \\ 0 & 0 & \bar{c}_W & \bar{s}_W \\ 0 & 0 & -\bar{s}_W & \bar{c}_W \end{bmatrix}, \quad V_{JK} = \begin{bmatrix} \frac{-i}{\sqrt{2}} & \frac{i}{\sqrt{2}} & 0 & 0 \\ \frac{1}{\sqrt{2}} & \frac{1}{\sqrt{2}} & 0 & 0 \\ 0 & 0 & -1 & 0 \\ 0 & 0 & 0 & 1 \end{bmatrix}. \quad (5)$$

104 \mathcal{U} and \mathcal{V} transform the weak eigenstate basis fields, W and ϕ , to the physical basis fields
 105 $A^I = \{W^+, W^-, Z, A\}$ and $\Phi^I = \{\Phi^-, \Phi^+, \chi, h\}$. The barred Weinberg angles, \bar{s}_W and

106 \bar{c}_W are defined in the Appendix. In addition to the above we also have the ghosts for the
 107 electroweak gauge bosons, $u^A = \mathcal{U}_G^A u^C$, the gluon field G^A and the corresponding ghost
 108 u_G^A . The gluons and their corresponding ghosts are transformed to canonically normalized
 109 fields by:

$$G^A = \sqrt{\kappa^{-1}} \mathcal{G}^A, \quad u_G^A = \sqrt{\kappa^{-1}} u_G^A. \quad (6)$$

110 κ is defined below, and is the field space connection of the combination $\mathcal{G}_{\mu\nu}^A \mathcal{G}^{A,\mu\nu}$. Script
 111 latin indices are $SU(3)_c$ gluon indices. In this article, fermionic fields only occur in loops
 112 and are therefore always summed over, as such we use the short hand ψ for all fermionic
 113 fields.

114 The full set of operator forms contributing to two- and three-point functions of the
 115 SMEFT was derived in [10]. They include:

$$\begin{aligned} h_{IJ}(D_\mu\phi)^I(D_\mu\phi)^J, & \quad g_{AB}W_{\mu\nu}^A W^{B\mu\nu}, & \quad \kappa_{IJ}^A(D_\mu\phi)^I(D_\nu\phi)^J W_A^{\mu\nu}, \\ \mathcal{Y}\bar{\psi}_1\psi_2, & \quad \kappa_{AB}\mathcal{G}_{\mu\nu}^A \mathcal{G}^{A\mu\nu}, & \\ f_{ABC}W_{\mu\nu}^A W^{B,\nu\rho} W_\rho^{C,\mu}, & \quad d_A\bar{\psi}_1\sigma^{\mu\nu}\psi_2\mathcal{W}_{\mu\nu}^A, & \quad \kappa_{ABC}\mathcal{G}_{\nu\mu}^A \mathcal{G}^{B,\rho\nu} \mathcal{G}^{C,\mu\rho}, \\ c\bar{\psi}_1\sigma^{\mu\nu}T_A\psi_2\mathcal{G}_{\mu\nu}^A, & \quad L_{IA}\bar{\psi}\gamma^\mu\sigma_A\psi_2(D_\mu\phi)^I. & \end{aligned} \quad (7)$$

116 The covariant derivative of the four component scalar and the field strength tensors of the
 117 vectors are then defined as:

$$(D_\mu\phi)^I = \left(\partial^\mu\delta_J^I - \frac{1}{2}W^{A,\mu}\tilde{\gamma}_{A,J}^I \right) \phi^J, \quad (8)$$

$$W_{\mu\nu}^A = \partial_\mu W_\nu^A - \partial_\nu W_\mu^A - \tilde{\epsilon}^A{}_{BC}W_\mu^B W_\nu^C, \quad (9)$$

$$\mathcal{G}_{\mu\nu}^A = \partial_\mu \mathcal{G}_\nu^A - \partial_\nu \mathcal{G}_\mu^A - f^A{}_{BC}\mathcal{G}_\mu^B \mathcal{G}_\nu^C. \quad (10)$$

118 The matrices $\tilde{\gamma}_{A,J}^I$ and $\tilde{\epsilon}^A{}_{BC}$ are defined in the Appendix. The $f^A{}_{BC}$ are the usual structure
 119 constants of $SU(3)_c$.

120 In addition to the operators defined in Eq. 7 we also define the all-orders Higgs poten-
 121 tial,

$$V(\phi^I) = \frac{\lambda}{4}(\phi^2 - v_0^2)^2 - \sum_{n=1}^{\infty} c_H^{(4+2n)} \left(\frac{\phi^2}{2} \right)^{2+n}. \quad (11)$$

122 In the above, v_0 is the vacuum expectation value that minimizes the tree-level Higgs
 123 potential for the SM. Spontaneous symmetry breaking occurs in the geoSMEFT for $\phi^I \rightarrow$
 124 $v\delta^{I4} + \sqrt{h}^{IJ}V_{JK}\Phi^{K1}$, where v is the vacuum expectation value which minimizes the tree
 125 level potential of the geoSMEFT. $c_H^{(4+2n)}$ is the Wilson coefficient of the dimension $4+2n$
 126 pure Higgs operator suppressed by the heavy mass scale Λ^{2n} , this Λ dependence is absorbed
 127 into the Wilson coefficient here and for the operators below for convenience. At tree level,
 128 requiring the coefficient of the tadpole term in the potential be zero gives the relation
 129 between v_0 and v :

$$t = 0 \propto v^2 - \frac{1}{\lambda} \sum_{n=1}^{\infty} \frac{(4+2n)v^{2+2n}}{2^{2+n}} c_H^{(2n+4)} - v_0^2. \quad (12)$$

130 We note that solving this equation for v^2 requires numerical methods for $n \geq 4$ as it is a
 131 polynomial of order $n+1$ in v^2 .

¹This is a convenient choice of how to realize spontaneous symmetry breaking in the geoSMEFT which is consistent with $\langle H^\dagger H \rangle = v^2/2$ [12].

132 In what follows we will derive the one-loop correction to this result to all orders in the
 133 SMEFT power counting. The choice of $t = 0$ at one loop corresponds to the FJ tadpole
 134 scheme [13], with this choice we choose to expand about the true (one-loop) vacuum. This
 135 simplifying choice means tadpole diagrams need not be included in one-loop calculations
 136 (the tadpole and its counter term exactly cancel), however the loop improved vacuum
 137 expectation value needs to be used in tree level calculations. Further, this one-loop result
 138 is required to demonstrate the gauge invariance of observables, such as the masses of
 139 the gauge bosons in the on-shell renormalization scheme [14, 15]. This is discussed in
 140 Appendix B as well as in the conclusions.

141 The terms from Eq. 7 which contribute to the one-loop tadpole diagram are those which
 142 involve a single Higgs boson coupling to two fermions, gauge bosons, or additional scalars.
 143 As such the last two lines do not contribute as they include three or more particles other
 144 than the Higgs boson and therefore only contribute at higher loop order. In the case of the
 145 connection L_{IA} there is no contribution as these operators correspond to the Hermitian
 146 derivative form, $(H^\dagger \overleftrightarrow{D}_\mu H)(\bar{\psi}\gamma^\mu\psi)$, which causes the Higgs-fermion couplings to vanish
 147 identically. While the operators coupling the Higgs boson to gluons will result in scale-less
 148 loop integrals which vanish identically, we retain them as the all-orders Feynman rules
 149 derived from the κ_{AB} operator form are the simplest and serve as intuitive examples of
 150 how the rules are derived. Reproducing the all-orders form of the relevant connections
 151 from [10] we have:

$$h_{IJ} = \left[1 + \phi^2 c_{H\Box}^{(6)} + \sum_{n=0}^{\infty} \left(\frac{\phi^2}{2} \right)^{n+2} (c_{HD}^{(8+2n)} - c_{H,D2}^{(8+2n)}) \right] \delta_{IJ} \\ + \frac{\Gamma_{A,J}^I \phi_K \Gamma_{A,L}^K \phi^L}{2} \left(\frac{c_{HD}^{(6)}}{2} + \sum_{n=0}^{\infty} \left(\frac{\phi^2}{2} \right)^{n+1} c_{HD,2}^{(8+2n)} \right), \quad (13)$$

$$g_{AB} = \left[1 - 4 \sum_{n=0}^{\infty} (c_{HW}^{(6+2n)} (1 - \delta_{A4}) + c_{HB}^{(6+2n)} \delta_{A4}) \left(\frac{\phi^2}{2} \right)^{n+1} \right] \delta_{AB} \\ - \sum_{n=0}^{\infty} \left(\frac{\phi^2}{2} \right)^n (\phi_I \Gamma_{A,J}^I \phi^J) (\phi_L \Gamma_{B,K}^L \phi^K) (1 - \delta_{A4}) (1 - \delta_{B4}) \\ + \left[\sum_{n=0}^{\infty} c_{HWB}^{(6+2n)} \left(\frac{\phi^2}{2} \right)^n \right] [(\phi_I \Gamma_{A,J}^I \phi^J) (1 - \delta_{A4}) \delta_{B4} + (A \leftrightarrow B)], \quad (14)$$

$$\kappa_{IJ}^A = -\frac{1}{2} \gamma_{A,J}^I \delta_{A4} \sum_{n=0}^{\infty} c_{HDHB}^{(8+2n)} \left(\frac{\phi^2}{2} \right)^{n+1} - \frac{1}{2} \gamma_{A,J}^I (1 - \delta_{A4}) \sum_{n=0}^{\infty} c_{HDHW}^{(8+2n)} \left(\frac{\phi^2}{2} \right)^{n+1} \\ - \frac{1}{8} (1 - \delta_{A4}) [\phi_K \Gamma_{A,L}^K \phi^L] [\phi_M \Gamma_{B,L}^M \phi^N] \gamma_{B,J}^I \sum_{n=0}^{\infty} c_{HDHW,3}^{(10+2n)} \left(\frac{\phi^2}{2} \right)^n \\ + \frac{1}{4} \epsilon_{ABC} [\phi_K \Gamma_{B,L}^K \phi^L] \gamma_{C,J}^I \sum_{n=0}^{\infty} c_{HDHW,2}^{(8+2n)} \left(\frac{\phi^2}{2} \right)^n, \quad (15)$$

$$\mathcal{Y}_{pr}^\psi = -\overset{(\sim)}{H}(\phi_I)[Y_\psi]^\dagger + \overset{(\sim)}{H}(\psi_I) \sum_{n=0}^{\infty} c_{\psi H,pr}^{(6+2n)} \left(\frac{\phi^2}{2} \right)^{n+1}, \quad (16)$$

$$\kappa_{AB} = \left[1 - 4 \sum_{n=0}^{\infty} c_{HG}^{(6+2n)} \left(\frac{\phi^2}{2} \right)^{n+1} \right] \delta_{AB} \rightarrow \kappa \equiv \left[1 - 4 \sum_{n=0}^{\infty} c_{HG}^{(6+2n)} \left(\frac{\phi^2}{2} \right)^{n+1} \right]. \quad (17)$$

152

153 The matrices $\Gamma_{A,J}^I$ and $\gamma_{A,J}^I$ are given in the Appendix for brevity. We have also used
 154 $\phi^2 = \phi^I \phi_I = \phi_I \delta^{IJ} \phi_J$. The $c_i^{(n)}$ are the Wilson coefficients of operators of dimension n
 155 and are suppressed by a factor of Λ^{n-4} which has been absorbed into their definition for

156 the sake of compactness of these and the following expressions. The inverse-square root
 157 of g_{IJ} and h_{IJ} are the matrices of Eq. 4 which with the matrices U and V take the weak
 158 eigenstate fields to the mass eigenstate fields of the SMEFT.

159 The above is all that is needed to define the relevant all-orders three-point functions
 160 for the classical Lagrangian in the geoSMEFT:

$$\begin{aligned} \mathcal{L}_{\text{cl}}(\phi^I, W^A, \mathcal{G}^A, \psi) = & h_{IJ}(D_\mu\phi)^I(D_\mu\phi)^J - V(\phi) + g_{AB}W_{\mu\nu}^A W^{B,\mu\nu} + \kappa\mathcal{G}_{\mu\nu}^A \mathcal{G}^{A,\mu\nu} \\ & + \kappa_{IJ}^A (D_\mu\phi)^I (D_\nu\phi)^J W_A^{\mu\nu} + \sum_{\psi} \mathcal{Y}\bar{\psi}_1\psi_2. \end{aligned} \quad (18)$$

161 In Section 4 we will choose to adopt the background field method of gauge fixing. Therefore
 162 in the discussion of the classical Lagrangian that follows we will double the bosonic field
 163 content of the above Lagrangian as:

$$\mathcal{L}_{\text{cl}}(\phi^I, W_\mu^A, \mathcal{G}_\mu^A, \psi) \rightarrow \mathcal{L}_{\text{cl}}(\phi^I + \hat{\phi}^I, W^A + \hat{W}^A, \mathcal{G}^A + \hat{\mathcal{G}}^A, \psi). \quad (19)$$

164 The choice of the background field method has various advantages, one of which is the
 165 preservation of the naive Ward Identities as discussed in [12, 16, 17]. This methodology
 166 has been adopted in many SMEFT related publications because of its nice properties, see
 167 for example [7, 18, 19]. In this methodology all external particles for a given amplitude
 168 correspond to background field while internal lines are quantum fields. Therefore in what
 169 follows we derive the couplings \hat{h} to two quantum fields.

170 3 The all-orders vertices

171 In order to define the relevant three-point functions for the one-loop tadpole diagrams
 172 we must obtain the relevant Feynman rules from Eq. 7. We will do this while preserving
 173 the form of the field-space connections when possible in order to maintain results that
 174 are manifestly all orders in the $\frac{1}{\Lambda^n}$ power counting. The Feynman rules that follow were
 175 checked using `FeynRules` and are written in the `FeynRules` output format, i.e. the sub-
 176 script of a field in $\{\}$ corresponds to the momenta, Lorentz indices, and color indices with
 177 the same subscript on the right side of the equations below.

178 The simplest Feynman rules to derive are from the field space connections g_{AB} , κ_{AB} ,
 179 and Y_{pr}^ψ as the Higgs dependence is purely in the connection matrix. Varying Eq. 17 with
 180 respect to the background field \hat{h} gives the coupling of a Higgs boson to two gluons:

$$\{\hat{h}, G_1, G_2\} = i \left\langle \frac{\delta\kappa}{\delta\hat{h}} \right\rangle \left(\sqrt{\kappa^{-1}} \right)^2 (p_1^{\mu_2} p_2^{\mu_1} - p_1 \cdot p_2 \eta^{\mu\nu}) \delta^{A_1 A_2}. \quad (20)$$

181 It should be noted there are implied rotations of the quantity ϕ_I within the field-space
 182 connections such as κ : beyond leading order $\sqrt{\kappa}$ is a function of $\phi^I = \sqrt{h}^{IJ} V_{JK} \Phi^K$.
 183 Explicitly taking the variations gives instead:

$$\{\hat{h}, G_1, G_2\} \rightarrow i\sqrt{h}^{44} \left(\sqrt{\kappa^{-1}} \right)^2 v_T \sum_{i=0}^{\infty} \frac{v_T^{2n} (n+1)}{2^{n-2}} c_{HG}^{(6+2n)} \Pi_{1,2} \delta^{A_1 A_2}. \quad (21)$$

184 Where, for convenience, we have defined,

$$\Pi_{1,2} \equiv (p_1^{\mu_2} p_2^{\mu_1} - p_1 \cdot p_2 \eta^{\mu_1 \mu_2}). \quad (22)$$

185 Similarly for the yukawa-like couplings:

$$\{\hat{h}, \bar{\psi}_r, \psi_r\} = -i \left\langle \frac{\delta \mathcal{Y}_{rr}^\psi}{\delta \hat{h}} \right\rangle \quad (23)$$

$$= i \frac{\sqrt{h}^{44}}{v} \bar{M}_{\psi,pp} - i \frac{\sqrt{h}^{44}}{\sqrt{2}} \sum_{n=0}^{\infty} c_{\psi H,pp}^{(6+2n)} \frac{v^{2n+2}}{2^{n+1}} (2n+2). \quad (24)$$

186 As only like-flavors will contribute to the Tadpole diagram we have only considered diagonal entries of \mathcal{Y}^ψ and substituted in terms of the barred tree-level masses of the fermions.
187
188 The tree-level fermion mass to all orders is simply the expectation of the field connection
189 \mathcal{Y} of Eq. 16:

$$\bar{M}_\psi = \langle (\mathcal{Y}^\psi)^\dagger \rangle. \quad (25)$$

190 The remaining terms are more complicated than the above, as such we only write the
191 vertex functions in terms of variations on the field-space connections. Some examples of
192 the field-space connections expanded in terms of Wilson coefficients can be found in the
193 Appendix. The coupling to two gauge bosons coming from g_{AB} is given by:

$$\{\hat{h}, W_1^+, W_2^-\} = -i \left\langle \frac{\delta g_{11}}{\delta \hat{h}} \right\rangle (\sqrt{g}^{11})^2 \Pi_{1,2}, \quad (26)$$

$$\{\hat{h}, A_1, A_2\} = -i \Sigma_{AA} \Pi_{1,2}, \quad (27)$$

$$\{\hat{h}, Z_1, Z_2\} = -i \Sigma_{ZZ} \Pi_{1,2}, \quad (28)$$

$$\Sigma_{AA} \equiv \sum_{i,j=3}^4 \left(\bar{c}_W^2 \left\langle \frac{\delta g_{ij}}{\delta \hat{h}} \right\rangle \sqrt{g}^{i4} \sqrt{g}^{j4} + 2\bar{c}_W \bar{s}_W \left\langle \frac{\delta g_{ij}}{\delta \hat{h}} \right\rangle \sqrt{g}^{3i} \sqrt{g}^{j4} + \bar{s}_W^2 \left\langle \frac{\delta g_{ij}}{\delta \hat{h}} \right\rangle \sqrt{g}^{3i} \sqrt{g}^{3j} \right), \quad (29)$$

$$\begin{aligned} \Sigma_{ZZ} &\equiv \sum_{i,j=3}^4 \left(\bar{c}_W^2 \left\langle \frac{\delta g_{ij}}{\delta \hat{h}} \right\rangle \sqrt{g}^{3i} \sqrt{g}^{3j} - 2\bar{c}_W \bar{s}_W \left\langle \frac{\delta g_{ij}}{\delta \hat{h}} \right\rangle \sqrt{g}^{3i} \sqrt{g}^{j4} + \bar{s}_W^2 \left\langle \frac{\delta g_{ij}}{\delta \hat{h}} \right\rangle \sqrt{g}^{i4} \sqrt{g}^{j4} \right) \\ &= \Sigma_{AA} (\bar{s}_W \rightarrow -\bar{c}_W, \bar{c}_W \rightarrow \bar{s}_W). \end{aligned} \quad (30)$$

194

195 In order to form a tadpole diagram from the connection κ_{IJ}^A one of the covariant deriva-
196 tives must generate a vector boson while the other must correspond to the background
197 Higgs boson, as such the rules are straightforward to derive as well:

$$\begin{aligned} \{\hat{h}_1, W_2^+, W_3^-\} &= \bar{g}_2 \sqrt{g}^{11} \sqrt{h}^{44} v \left[(\langle \kappa_{13}^1 \rangle - i \langle \kappa_{14}^1 \rangle) p_1^{\mu_2} p_2^{\mu_3} - (\langle \kappa_{13}^1 \rangle + i \langle \kappa_{14}^1 \rangle) p_1^{\mu_3} p_3^{\mu_2} \right. \\ &\quad \left. + (\langle \kappa_{13}^1 \rangle [p_1 \cdot p_3 - p_1 \cdot p_2] + i \langle \kappa_{14}^1 \rangle [p_1 \cdot p_2 + p_1 \cdot p_3]) \eta^{\mu_2 \mu_3} \right], \end{aligned} \quad (31)$$

$$\begin{aligned} \{\hat{h}_1, Z_2, Z_3\} &= -i \sqrt{h}^{44} \bar{g}_{ZV} v \left[(\bar{c}_W \sqrt{g}^{33} - \bar{s}_W \sqrt{g}^{34}) \langle \kappa_{34}^3 \rangle + (\bar{s}_W \sqrt{g}^{44} - \bar{c}_W \sqrt{g}^{34}) \langle \kappa_{12}^4 \rangle \right] \\ &\quad \times [p_1^{\mu_2} p_2^{\mu_3} + p_1^{\mu_3} p_3^{\mu_2} - p_1 \cdot (p_2 + p_3) \eta^{\mu_2 \mu_3}]. \end{aligned} \quad (32)$$

198 No coupling to the photon is generated as one of the vector bosons must come from the
199 covariant derivative which has no A dependence for the Higgs boson. In simplifying these

200 expressions we have used:

$$\langle \kappa_{13}^1 \rangle = -\langle \kappa_{24}^1 \rangle = -\langle \kappa_{31}^1 \rangle = \langle \kappa_{42}^1 \rangle = \langle \kappa_{14}^2 \rangle = \langle \kappa_{23}^2 \rangle = -\langle \kappa_{32}^2 \rangle = -\langle \kappa_{41}^2 \rangle, \quad (33)$$

$$\langle \kappa_{14}^1 \rangle = \langle \kappa_{23}^1 \rangle = -\langle \kappa_{32}^1 \rangle = -\langle \kappa_{41}^1 \rangle = -\langle \kappa_{13}^2 \rangle = \langle \kappa_{24}^2 \rangle = \langle \kappa_{31}^2 \rangle = -\langle \kappa_{42}^2 \rangle, \quad (34)$$

$$\langle \kappa_{12}^3 \rangle = -\langle \kappa_{21}^3 \rangle, \quad (35)$$

$$\langle \kappa_{34}^3 \rangle = -\langle \kappa_{43}^3 \rangle, \quad (36)$$

$$\langle \kappa_{12}^4 \rangle = -\langle \kappa_{21}^4 \rangle = -\langle \kappa_{34}^4 \rangle = \langle \kappa_{43}^4 \rangle. \quad (37)$$

201 As the rules for interactions derived from κ_{IJ}^A necessarily depend on the momentum of the
202 background Higgs boson (i.e. one of the derivatives must be acting on the Higgs boson)
203 these rules will not contribute to the tadpole diagram.

204 Finally, the Feynman rules arising from the field-space connection h_{IJ} are slightly more
205 complicated as the background Higgs boson can come from either the metric or the $(D_\mu \phi)$
206 terms. These operator forms also contribute not only to Higgs-gauge couplings, but also
207 to Higgs-goldstone couplings. For \hat{h} sourced from the field space connection we have the
208 following rules:

$$\{\hat{h}, \Phi_1^0, \Phi_1^0\} = -i \left\langle \frac{\delta h_{33}}{\delta \hat{h}} \right\rangle (\sqrt{h}^{33})^2 p_1 \cdot p_2, \quad (38)$$

$$\{\hat{h}, \Phi_1^+, \Phi_2^-\} = -i \left\langle \frac{\delta h_{11}}{\delta \hat{h}} \right\rangle (\sqrt{h}^{11})^2 p_1 \cdot p_2, \quad (39)$$

$$\{\hat{h}, h_1, h_2\} = -i \left\langle \frac{\delta h_{44}}{\delta \hat{h}} \right\rangle (\sqrt{h}^{44})^2 p_1 \cdot p_2, \quad (40)$$

$$\{\hat{h}, W_1^+, W_2^-\} = i \left\langle \frac{\delta h_{11}}{\delta \hat{h}} \right\rangle \bar{M}_W^2 (\sqrt{h}^{11})^2 \eta_{\mu_1 \mu_2}, \quad (41)$$

$$\{\hat{h}, Z_1, Z_2\} = i \left\langle \frac{\delta h_{33}}{\delta \hat{h}} \right\rangle \bar{M}_Z^2 (\sqrt{h}^{33})^2 \eta_{\mu_1 \mu_2}. \quad (42)$$

209 The coupling $\hat{h}\gamma\gamma$ vanishes identically, which follows from the fact the operator forms
210 of the field-space connection h_{IJ} correspond to rescalings of the SM Higgs couplings to
211 vector bosons. In the case that \hat{h} is sourced from the covariant derivative terms we have
212 two contributions. The first is from the $\langle h \rangle$ which can only generate \hat{h} -vector three point
213 functions²:

$$\{\hat{h}, W_1^+, W_2^-\} = 2i\sqrt{h}^{44} \frac{\bar{M}_W^2}{v} \eta_{\mu_1 \mu_2}, \quad (43)$$

$$\{\hat{h}, Z_1, Z_2\} = 2i\sqrt{h}^{44} \frac{\bar{M}_Z^2}{v} \eta_{\mu_1 \mu_2}. \quad (44)$$

214 As above, the $\hat{h}\gamma\gamma$ coupling vanishes identically. Secondly, \hat{h} couplings to goldstone bosons
215 from variations of the metric with respect to the goldstone bosons could be present, how-
216 ever they vanish identically.

217 In addition to the above we need to include terms like $c_H^{(2n-4)}(H^\dagger H)^{2n}$. The Feynman
218 rules for \hat{h} coupling to two quantum fields can be generalized from Eq. 4.2 of [10] by using

²Also $\hat{h}\Phi^{0,\pm}$ -vector couplings which do not contribute to the Tadpole diagram.

219 the multinomial coefficient:

$$\{\hat{h}, h, h\} = -2i(\sqrt{h}^{44})^3 v \left[3\lambda - \sum_{n=3}^{\infty} \frac{1}{2^n} \binom{2n}{1, 2, 2n-3} v^{2n-4} c_H^{(2n)} \right], \quad (45)$$

$$\{\hat{h}, \Phi^0, \Phi^0\} = -2i(\sqrt{h}^{33})^2 \sqrt{h}^{44} v \left[\lambda - \sum_{n=3}^{\infty} \frac{1}{2^{n-1}} \binom{n}{1, 1, n-2} v^{2n-4} c_H^{(2n)} \right], \quad (46)$$

$$\{\hat{h}, \Phi^+, \Phi^-\} = -i(\sqrt{h}^{11})^2 \sqrt{h}^{44} v \left[2\lambda - \sum_{n=3}^{\infty} \frac{1}{2^{n-2}} \binom{n}{1, 1, n-2} v^{2n-4} c_H^{(2n)} \right]. \quad (47)$$

220 In the above the multinomial for $\hat{h}h^2$ can be understood to come from $(v + \hat{h} + h)^{2n}$ terms,
 221 the Φ^0 rule from $[(\Phi^0)^2 + 2\hat{h}v + v^2]^n$, and the rule for Φ^\pm from $[2|\Phi^\pm|^2 + 2\hat{h}v + v^2]^n$. This
 222 explains the minor differences between the Feynman rules above.

223 The above constitute all the rules from the classical Lagrangian necessary to perform
 224 the calculation of the tadpole diagrams to all orders in the SMEFT power counting, what
 225 remains are the gauge-fixing and ghost contributions.

226 4 Gauge fixing the geoSMEFT

227 Background gauge fixing for the SMEFT was performed first in [9]. This was first done for
 228 the gluons in [18], then later repeated in [16] in a manner more consistent with the gauge
 229 fixing of the weak gauge bosons of [9] which is adopted here. The gauge fixing terms are
 230 given by:

$$\mathcal{L}_{GF} = -\frac{\hat{g}_{AB}}{2\xi_W} \mathcal{G}^A \mathcal{G}^B - \frac{\kappa}{2\xi_G} G_{\text{color}}^A G_{\text{color}}^A, \quad (48)$$

$$\mathcal{G}^A = \partial_\mu W^{A,\mu} - \tilde{e}^A_{BC} \hat{W}_\mu^B W^{C\mu} + \frac{\xi}{2} \hat{g}^{AB} \phi^I \hat{h}_{IK} \tilde{\gamma}_{B,J}^K \hat{\phi}^J, \quad (49)$$

$$G_{\text{color}}^A = \partial_\mu G^{\mu,A} - g_3 f^{ABC} \hat{G}_{\mu,B} G_C^\mu. \quad (50)$$

231 Where in the above, unhatted fields are understood to be quantum fields and the hatted
 232 field-space connections are the normal field space connections with all quantum fields set
 233 to zero. This notational choice is also the case below in the ghost Lagrangian. Starting
 234 with the gluonic gauge fixing as it is the simplest we obtain the Feynman rule:

$$\{\hat{h}, G_1, G_2\} = \frac{i}{\xi_G} \left\langle \frac{\delta \kappa}{\delta \hat{h}} \right\rangle (\sqrt{\kappa^{-1}})^2 p_1^{\mu_1} p_2^{\mu_2} \delta^{A_1 A_2}. \quad (51)$$

235 In the case of the electroweak gauge fixing a coupling of the background Higgs field to gauge
 236 bosons can be obtained from the variation with respect to the field-space connection of
 237 Eq. 48 and the square of the derivative term of Eq. 49. The second terms of Eqs. 49 and 50
 238 cannot contribute as they include a background gauge field, while the final term allows
 239 for a \hat{h} coupling to goldstone bosons when all but one of the \hat{g} , \hat{h} , and $\hat{\phi}$ are set to their

240 expectation values. This results in the following Feynman Rules:

$$\{\hat{h}, W_1^+, W_2^-\} = \frac{i}{\xi} \left\langle \frac{\delta g_{11}}{\delta \hat{h}} \right\rangle (\sqrt{g^{11}})^2 p_1^{\mu_1} p_2^{\mu_2}, \quad (52)$$

$$\{\hat{h}, A_1, A_2\} = \frac{i}{\xi} \Sigma_{AA} p_1^{\mu_1} p_2^{\mu_2}, \quad (53)$$

$$\{\hat{h}, Z_1, Z_2\} = \frac{i}{\xi} \Sigma_{ZZ} p_1^{\mu_1} p_2^{\mu_2}, \quad (54)$$

$$\{\hat{h}, \Phi^+, \Phi^-\} = -i \frac{\bar{M}_W^2}{v} \left[2 \left\langle \frac{\delta h_{11}}{\delta \hat{h}} \right\rangle (\sqrt{h^{11}})^2 v + 2\sqrt{h^{44}} + \left\langle \frac{\delta g^{11}}{\delta \hat{h}} \right\rangle (\sqrt{g_{11}})^2 v \right] \xi_W \quad (55)$$

$$\{\hat{h}, \Phi^0, \Phi^0\} = -i \frac{\bar{M}_Z^2}{v} \left[2 \left\langle \frac{\delta h_{33}}{\delta \hat{h}} \right\rangle (\sqrt{h^{33}})^2 v + 2\sqrt{h^{44}} - \Sigma_{ZZ} v \right] \xi_W. \quad (56)$$

$$(57)$$

241 Note no \hat{h} coupling to two quantum Higgs bosons is generated.

242 The ghost Lagrangian was also derived in [9]³, it is reproduced here excluding any
243 terms with gauge fields as they cannot contribute to the one-loop Tadpole diagram (the
244 ghost Lagrangian is by definition quadratic in the ghost fields):

$$\mathcal{L}_{\text{ghost}} = -\hat{g}_{AB} \bar{u}^B \left[\partial^2 + \frac{\xi}{4} \hat{g}^{AD} (\phi^J + \hat{\phi}^J) \tilde{\gamma}_{CJ}^I \hat{h}_{IK} \tilde{\gamma}_{DL}^K \hat{\phi}^L \right] u^C - \hat{\kappa} \bar{u}_A^G \partial^2 u_A^G. \quad (58)$$

245 As was the case for the gauge fixing terms, $\hat{h}\bar{u}u$ couplings can be obtained either from a
246 variation with respect to one of the field-space connections or explicitly from $\hat{\phi}$, \hat{h} , or \hat{g} :

$$\{\hat{h}, \bar{u}_1^G, u_2^G\} = i \left\langle \frac{\delta \kappa}{\delta \hat{h}} \right\rangle (\sqrt{\kappa^{-1}})^2 p_2^2 \delta_{A_1 A_2}, \quad (59)$$

$$\{\hat{h}, \bar{u}_1^{W^+}, u_2^{W^+}\} = -i \left[\left\langle \frac{\delta h_{11}}{\delta \hat{h}} \right\rangle \bar{M}_W^2 (\sqrt{h^{11}})^2 \xi + 2\bar{M}_W^2 \sqrt{h^{44}} \xi - (\sqrt{g^{11}})^2 \left\langle \frac{\delta g_{11}}{\delta \hat{h}} \right\rangle p_2^2 \right] \quad (60)$$

$$= \{\hat{h}, \bar{u}_1^{W^-}, u_2^{W^-}\}, \quad (61)$$

$$\{\hat{h}, \bar{u}_1^A, u_2^A\} = i \Sigma_{AA} p_2^2,$$

$$\{\hat{h}, \bar{u}_1^Z, u_2^Z\} = i \Sigma_{ZZ} p_2^2 - i \bar{M}_Z^2 \left(2\sqrt{h^{44}} + (\sqrt{h^{33}})^2 \left\langle \frac{\delta h_{33}}{\delta \hat{h}} \right\rangle \right) \xi. \quad (62)$$

247 In the case of the ghosts associated with the photon, the ξ dependent term vanishes
248 identically. This is analogous to the case of the classical contribution from the field space
249 metric h_{IJ} , see the discussions around Eqs. 42 and 44. With the above, all Feynman rules
250 necessary to calculate the tadpole diagram at one loop and to all orders in the SMEFT
251 expansion are now defined.

252 5 The all-orders SMEFT tadpole

253 The one loop diagrams that contribute are shown in Figure 1, as was noted in Section 2
254 the Feynman rules coupling the Higgs boson to gluons as well as those coupling the Higgs
255 boson to colored ghosts do not contribute to the tadpole diagram as the loop integral is

³Here we have adopted the sign choice of [18].

256 scaleless. Making use of dimensional regularization in $d = 4 - 2\epsilon$ dimensions, the fermionic
257 couplings result in the following contribution at one loop:

$$T_H^\psi = -\frac{N_c \bar{M}_\psi}{4\pi^2} \left\langle \frac{\delta \mathcal{Y}^\psi}{\delta \hat{h}} \right\rangle A_0(\bar{M}_\psi) \quad (63)$$

$$= \frac{N_c \bar{M}_\psi}{4\pi^2} \sqrt{h}^{44} \left(\frac{\bar{M}_\psi}{v} - \frac{1}{\sqrt{2}} \sum_{n=0}^{\infty} \frac{v^{2n+2}}{2^{n+1}} (2n+2) \right) A_0(\bar{M}_\psi) \quad (64)$$

$$= \frac{N_c \bar{M}_\psi}{4\pi^2} \left[\frac{\bar{M}_\psi}{v} - \frac{v}{4} \left(2\sqrt{2} v c_{\psi H}^{(6)} + \bar{M}_\psi [c_{HD}^{(6)} - 4c_{H\Box}] \right) - \frac{v^4}{8} \sqrt{2} \left(c_{\psi H}^{(8)} + [4c_{H\Box}^{(6)} - c_{HD}^{(6)}] c_{\psi H}^{(6)} \right) \right. \\ \left. + \frac{\bar{M}_\psi}{32} \left(4c_{HD}^{(8)} + 4c_{HD,2}^{(8)} - 3[c_{HD}^{(6)} - 4c_{H\Box}^{(6)}]^2 \right) \right] A_0(\bar{M}_\psi) + \mathcal{O}\left(\frac{1}{\Lambda^6}\right). \quad (65)$$

258 Where we have used the Passarino-Veltman scalar A function,

$$A_0(M) = M^2 \left[1 + \frac{1}{\epsilon} - \gamma_E + \log\left(\frac{4\pi\mu^2}{M^2}\right) \right]. \quad (66)$$

259 The three equivalences of Eq. 65 show first the geoSMEFT result, the result with the
260 variation of the field-space connection written explicitly in terms of the relevant Wilson
261 coefficients while keeping the compact form for the transformations that canonically nor-
262 malizes the Higgs background field, and finally the full expansion in terms of the Wilson
263 coefficients to order $\frac{1}{\Lambda^4}$. The barred quantities are not expanded as they are more closely
264 related to input parameters that would be chosen in a phenomenological study, this also
265 serves to simplify the expressions so they fit in paper format. This demonstrates that the
266 geoSMEFT trivially sums the Wilson coefficient dependence of the SMEFT. In a tradi-
267 tional SMEFT approach one would enumerate all the contributing operators to a given
268 order in the SMEFT power counting and the corresponding Feynman rules, perform the
269 calculations, and again expand to a given order. Here we perform the all orders calculation
270 and can expand to a given order after the full calculation is performed.

271 The compactness of the expressions also allows for a cleaner understanding of cancel-
272 lations in the theory such as in the case of cancellations between gauge-boson, ghost, and
273 goldstone boson contributions as we see next. Below we neglect to expand in terms of
274 individual Wilson coefficients until the terms are added together as many simplifications
275 occur after summing the diagrams. In the case of the W and Z bosons we have:

$$T_H^W = \frac{\bar{M}_W^2}{16\pi^2} \left[(\sqrt{g}^{-11})^2 \left\langle \frac{\delta g_{11}}{\delta \hat{h}} \right\rangle - \frac{2}{v} \sqrt{h}^{44} - \left\langle \frac{\delta h_{11}}{\delta \hat{h}} \right\rangle (\sqrt{h}^{11})^2 \right] \left[2\bar{M}_W^2 - 3A_0(\bar{M}_W) - \xi_W A_0(\sqrt{\xi_W} \bar{M}_W) \right], \quad (67)$$

$$T_H^Z = \frac{\bar{M}_Z^2}{32\pi^2} \left[\Sigma_{ZZ} - \frac{2}{v} \sqrt{h}^{44} - \left\langle \frac{\delta h_{33}}{\delta \hat{h}} \right\rangle (\sqrt{h}^{33})^2 \right] \left[2\bar{M}_Z^2 - 3A_0(\bar{M}_Z) - \xi A_0(\sqrt{\xi} \bar{M}_Z) \right]. \quad (68)$$

276

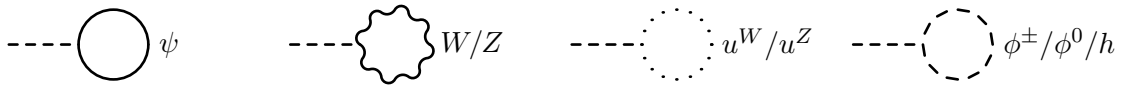


Figure 1: One loop diagrams contributing to the Tadpole. The photon and gluons and their corresponding ghosts do not contribute as they are massless the loop integrals are identically zero.

277 The ghost terms give (again, as the photon ghost term is scaleless the contribution is
278 identically zero):

$$T_H^{u^\pm} = \frac{\bar{M}_W^2}{8\pi^2} \left[\left\langle \frac{\delta g_{11}}{\delta \hat{h}} \right\rangle (\sqrt{g^{11}})^2 - \frac{2}{v} \sqrt{h^{44}} - \left\langle \frac{\delta h_{11}}{\delta \hat{h}} \right\rangle (\sqrt{h^{11}})^2 \right] \xi_W A_0(\sqrt{\xi_W} \bar{M}_W), \quad (69)$$

$$T_H^{u^Z} = \frac{\bar{M}_Z^2}{16\pi^2} \left[\Sigma_{ZZ} - \frac{2}{v} \sqrt{h^{44}} - \left\langle \frac{\delta h_{33}}{\delta \hat{h}} \right\rangle (\sqrt{h^{33}})^2 \right] \xi_W A_0(\sqrt{\xi_W} \bar{M}_Z), \quad (70)$$

279 and for the goldstone bosons we find:

$$T_H^{\Phi^\pm} = \frac{\bar{M}_W^2}{16\pi^2} \left[\frac{2}{v} \sqrt{h^{44}} + \left\langle \frac{\delta h_{11}}{\delta \hat{h}} \right\rangle (\sqrt{h^{11}})^2 + \left\langle \frac{\delta g^{11}}{\delta \hat{h}} \right\rangle (\sqrt{g^{11}})^2 \right] \xi_W A_0(\sqrt{\xi_W} \bar{M}_W) \quad (71)$$

$$+ \frac{v}{32\pi^2} (\sqrt{h^{11}})^2 \sqrt{h^{44}} \left(4\lambda - \sum_{n=3}^{\infty} \frac{1}{2^{n-3}} \binom{n}{1, 1, n-2} v^{2n-4} c_H^{(2n)} \right) A_0(\sqrt{\xi_W} \bar{M}_W),$$

$$T_H^{\Phi^0} = \frac{\bar{M}_Z^2}{32\pi^2} \left[\frac{2}{v} \sqrt{h^{44}} + \left\langle \frac{\delta h_{33}}{\delta \hat{h}} \right\rangle (\sqrt{h^{33}})^2 - \Sigma_{ZZ} \right] \xi_W A_0(\sqrt{\xi_W} \bar{M}_Z) \quad (72)$$

$$+ \frac{v}{64\pi^2} (\sqrt{h^{33}})^2 \sqrt{h^{44}} \left(4\lambda - \sum_{n=3}^{\infty} \frac{1}{2^{n-3}} \binom{n}{1, 1, n-2} v^{2n-4} c_H^{(2n)} \right) A_0(\sqrt{\xi} \bar{M}_Z).$$

280

281 Noting the raised indices in δg^{11} for the Φ^\pm contribution, we see that the ξ_W dependent
282 parts of the W and Z loops are cancelled exactly by the ghost and goldstone terms,
283 and only the λ and $c_H^{(n)}$ gauge-parameter dependent terms remain for the scalars. This
284 is exactly as was found for the SM Tadpole in the background field methodology [7].
285 Interestingly, the behavior goes beyond the SM-like interactions and also holds for the
286 interactions which only occur in the SMEFT, i.e. those proportional to δg and δh , as
287 well. This also means that the λ and $c_H^{(n)}$ terms are gauge dependent and therefore so is
288 the tadpole. This is also consistent with [7], where they found this dependence exactly
289 cancels against that of the Higgs two-point function and the loop contributions in the
290 process $H \rightarrow \gamma\gamma$ at order $\frac{1}{\Lambda^2}$ in the SMEFT, leaving the observable process $H \rightarrow \gamma\gamma$ gauge
291 invariant as it must be.

292 The sum of the vectors, ghosts, and goldstone bosons, neglecting λ and $c_H^{(n)}$ dependence
293 is given by:

$$T_H^{V,u,\Phi} = \frac{\bar{M}_W^2}{16\pi^2} \left[(\sqrt{g^{11}})^2 \left\langle \frac{\delta g_{11}}{\delta \hat{h}} \right\rangle - \frac{2}{v} \sqrt{h^{44}} - \left\langle \frac{\delta h_{11}}{\delta \hat{h}} \right\rangle (\sqrt{h^{11}})^2 \right] [2\bar{M}_W^2 - 3A_0(\bar{M}_W)]$$

$$+ \frac{\bar{M}_Z^2}{32\pi^2} \left[\Sigma_{ZZ} - \frac{2}{v} \sqrt{h^{44}} - \left\langle \frac{\delta h_{33}}{\delta \hat{h}} \right\rangle (\sqrt{h^{33}})^2 \right] [2\bar{M}_Z^2 - 3A_0(\bar{M}_Z)]. \quad (73)$$

294 In order to demonstrate the compactness of this expression we expand the quantity in
295 brackets for the W contribution to $\mathcal{O}(1/\Lambda^4)$ in terms of the Wilson coefficients:

$$\left[(\sqrt{g^{11}})^2 \left\langle \frac{\delta g_{11}}{\delta \hat{h}} \right\rangle - \frac{2}{v} \sqrt{h^{44}} - \left\langle \frac{\delta h_{11}}{\delta \hat{h}} \right\rangle (\sqrt{h^{11}})^2 \right] = -\frac{1}{v} \left[2 + \frac{v^2}{2} \left(c_{H\Box}^{(6)} - c_{HD}^{(6)} + 8c_{HW}^{(6)} \right) \right.$$

$$\left. + \frac{v^4}{16} \left(12c_{HD}^{(8)} - 20c_{HD,2}^{(8)} + 64c_{HW}^{(8)} + 3(c_{HD}^{(6)} - 4c_{H\Box}^{(6)})^2 + 16(4c_{H\Box}^{(6)} - c_{HD}^{(6)})c_{HW}^{(6)} + 128c_{HW}^{(6)} \right) \right]. \quad (74)$$

296

297 In the case of the Z contribution the result depends on many more operator coefficients,
298 as well as the the barred mixing angles due to the dependence in Σ_{ZZ} .

299 The last remaining contribution is from the quantum Higgs boson, which gives:

$$T_H^h = \frac{1}{32\pi^2} (\sqrt{h^{44}})^2 \left[\bar{M}_H^2 \left\langle \frac{\delta h_{44}}{\delta \hat{h}} \right\rangle + v \sqrt{h^{44}} \left(6\lambda - \sum_{n=3}^{\infty} \frac{1}{2^{n-1}} \binom{2n}{1, 2, 2n-3} v^{2n-4} c_H^{(2n)} \right) \right] A_0(\bar{M}_H). \quad (75)$$

300 The sum off all of the above contributions to T_H in the SM limit agrees with [7], providing
301 a useful cross check of the result. To the extent of the authors knowledge the $1/\Lambda^2$ result
302 does not exist in the literature in the background formalism.

303 With all of the contributions included we can then choose a renormalization condition
304 related to the tadpole. Returning to Eq. 11 we obtain the coefficient of the tadpole term:

$$t \equiv \frac{\sqrt{h^{44}} v}{16} \left[16\lambda(v_0^2 - v^2) + \sum_{n=1}^{\infty} \frac{(4+2n)v^{4+2n-1}}{2^{2+n}} c_H^{(4+2n)} \right]. \quad (76)$$

305 Choosing $t = 0$ corresponds to the proper ground state [13, 14] and is the scheme we
306 choose here. At tree level this simply reproduces the condition in Eq. 12. At one loop
307 this corresponds to cancelling the entire tadpole contribution. Introducing δt as a counter
308 term, we have the renormalization condition,

$$t = t_0 - \delta t = 0, \quad (77)$$

309 where t_0 corresponds to the tree level contribution. Choosing $t = 0$ corresponds to:

$$\begin{aligned} \delta t &= -T_H \\ &= + \sum_{\psi} \frac{N_c \bar{M}_{\psi}}{4\pi^2} \left\langle \frac{\delta \mathcal{Y}^{\psi}}{\delta \hat{h}} \right\rangle A_0(\bar{M}_{\psi}) \\ &\quad - \frac{\bar{M}_W^2}{16\pi^2} \left[(\sqrt{g^{11}})^2 \left\langle \frac{\delta g_{11}}{\delta \hat{h}} \right\rangle - \frac{2}{v} \sqrt{h^{44}} - \left\langle \frac{\delta h_{11}}{\delta \hat{h}} \right\rangle (\sqrt{h^{11}})^2 \right] [2\bar{M}_W^2 - 3A_0(\bar{M}_W)] \\ &\quad - \frac{\bar{M}_Z^2}{32\pi^2} \left[\Sigma_{ZZ} - \frac{2}{v} \sqrt{h^{44}} - \left\langle \frac{\delta h_{33}}{\delta \hat{h}} \right\rangle (\sqrt{h^{33}})^2 \right] [2\bar{M}_Z^2 - 3A_0(\bar{M}_Z)] \\ &\quad - \frac{v}{32\pi^2} (\sqrt{h^{11}})^2 \sqrt{h^{44}} \left(4\lambda - \sum_{n=3}^{\infty} \frac{1}{2^{n-3}} \binom{n}{1, 1, n-2} v^{2n-4} c_H^{(2n)} \right) A_0(\sqrt{\xi_W} \bar{M}_W) \\ &\quad - \frac{v}{64\pi^2} (\sqrt{h^{33}})^2 \sqrt{h^{44}} \left(4\lambda - \sum_{n=3}^{\infty} \frac{1}{2^{n-3}} \binom{n}{1, 1, n-2} v^{2n-4} c_H^{(2n)} \right) A_0(\sqrt{\xi_Z} \bar{M}_Z) \\ &\quad - \frac{1}{32\pi^2} (\sqrt{h^{44}})^2 \left[\bar{M}_H^2 \left\langle \frac{\delta h_{44}}{\delta \hat{h}} \right\rangle + v \sqrt{h^{44}} \left(6\lambda - \sum_{n=3}^{\infty} \frac{1}{2^{n-1}} \binom{2n}{1, 2, 2n-3} v^{2n-4} c_H^{(2n)} \right) \right] A_0(\bar{M}_H). \end{aligned} \quad (78)$$

310 which depends on four barred masses (counting the barred fermion mass only once), four
311 field-space connections plus Σ_{ZZ} , λ , and the sum over $c_H^{(n)}$. Treating the sums as a
312 single entity gives a total dependence on eleven quantities. Conversely, the standard
313 model result depends on four masses and λ . Expanding the tadpole result in terms of
314 the Wilson coefficients of the SMEFT and maintaining barred mass dependence instead
315 gives 12 parameters at dimension six and 21 at $\mathcal{O}(1/\Lambda^4)$ with 9 additional parameters at
316 each subsequent order⁴. In this context the geSMEFT represents a clear calculational
317 advantage over the traditional approach to the SMEFT.

⁴The number of new parameters in h_{IJ} , g_{AB} , and \mathcal{Y} at a given dimension above six stays constant, see Table 1 of [10].

318 Further, as we saw in the discussion about the gauge, goldstone, and ghost terms, the
319 compactness of the geoSMEFT expressions allows for a straightforward cancellation of
320 terms which would be unclear when expanded in terms of the many Wilson coefficients
321 contributing to each process. Similar simplifications of expressions can be expected for
322 higher n -point functions, and as these expressions will generally be more complicated
323 than those of the tadpole this simplification is crucial to an analytic understanding of the
324 SMEFT expansion at one loop.

325 6 Conclusions

326 We have constructed the Feynman rules necessary for the calculation of the tadpole di-
327 agram within the framework of the geoSMEFT. In doing so we have included, for the
328 first time, the gauge fixing of the geoSMEFT and the all-orders Feynman rules related to
329 gauge fixing which include a single background Higgs boson and two other particles. We
330 proceeded to calculate all diagrams contributing to the process. The results allowed us
331 to fix the minimum of the Higgs potential at one loop and to all orders in the SMEFT
332 power counting. In doing so we demonstrated the simplicity of expressions obtained in the
333 geoSMEFT as compared with those expanded in terms of the Wilson coefficients which is
334 necessary in standard approaches to the SMEFT. Further we obtained not only the first
335 one-loop calculation including full next to leading order results in the SMEFT, but the
336 first one-loop calculation including all orders contributions in $1/\Lambda^n$. As discussed in the
337 introduction and Appendix B, the tadpole diagram is not only essential to fully defining
338 one-loop results, such as the masses of the gauge bosons, but is also essential for the gauge
339 invariance of the theory at one loop. This demonstrates the foundational nature of this
340 work toward future precision calculations in the geoSMEFT.

341 Beyond the scope of the calculations contained in this article, we note that the geoSMEFT
342 is currently defined to include vertices of up to any three particles accompanied by arbi-
343 trarily many scalar field insertions. This has presented the opportunity for many all-orders
344 results at tree level [6, 11] and their projection to order $1/\Lambda^4$ in phenomenological studies.
345 This allows for the possibility to perform a truncation error analysis more consistent with
346 the SMEFT than those commonly used where partial dimension-six squared results are
347 used to estimate the truncation error. While few additional one-loop calculations are cur-
348 rently possible in the framework of the geoSMEFT, it is possible to systematically extend
349 the geoSMEFT to include any N particles plus arbitrarily many scalar field insertions.
350 This will allow for the all orders in $1/\Lambda^n$ calculation of all two-point functions in the near
351 future and subsequently higher n -point functions. With all orders results at tree- and
352 one-loop level we can then define a fully consistent truncation error associated with the
353 SMEFT. This is an important step toward a precision program for the studies at the High
354 Luminosity LHC as well as for supporting and informing the case for next generation
355 colliders.

356

357 Acknowledgements

358 TC thanks M. Trott, A. Martin, and J. Talbert for useful discussions and their reading of
359 the manuscript.

360 **Funding information** TC acknowledges funding from European Union's Horizon 2020
361 research and innovation program under the Marie Skłodowska-Curie grant agreement No.
362 890787.

363 A Useful geoSMEFT definitions and relations

364 The following definitions and geometric relations are used extensively throughout this
 365 work in order to simplify expressions and retain them in the geometric formulation. These
 366 relations can be found in [10]. The following matrices are used to define the covariant
 367 derivatives, field strength tensors, and field-space connections:

$$\gamma_{1,J}^I = \begin{bmatrix} 0 & 0 & 0 & -1 \\ 0 & 0 & -1 & 0 \\ 0 & 1 & 0 & 0 \\ 1 & 0 & 0 & 0 \end{bmatrix}, \quad \gamma_{2,J}^I = \begin{bmatrix} 0 & 0 & 1 & 0 \\ 0 & 0 & 0 & -1 \\ -1 & 0 & 0 & 0 \\ 0 & -1 & 0 & 0 \end{bmatrix}, \quad (79)$$

$$\gamma_{3,J}^I = \begin{bmatrix} 0 & -1 & 0 & 0 \\ 1 & 0 & 0 & 0 \\ 0 & 0 & 0 & -1 \\ 0 & 0 & 1 & 0 \end{bmatrix}, \quad \gamma_{4,J}^I = \begin{bmatrix} 0 & -1 & 0 & 0 \\ 1 & 0 & 0 & 0 \\ 0 & 0 & 0 & 1 \\ 0 & 0 & -1 & 0 \end{bmatrix}, \quad (80)$$

369 as well as:

$$\Gamma_{1,J}^I = \begin{bmatrix} 0 & 0 & 1 & 0 \\ 0 & 0 & 0 & -1 \\ 1 & 0 & 0 & 0 \\ 0 & -1 & 0 & 0 \end{bmatrix}, \quad \Gamma_{2,J}^I = \begin{bmatrix} 0 & 0 & 0 & 1 \\ 0 & 0 & 1 & 0 \\ 0 & 1 & 0 & 0 \\ 1 & 0 & 0 & 0 \end{bmatrix}, \quad (81)$$

$$\Gamma_{3,J}^I = \begin{bmatrix} -1 & 0 & 0 & 0 \\ 0 & -1 & 0 & 0 \\ 0 & 0 & 1 & 0 \\ 0 & 0 & 0 & 1 \end{bmatrix}, \quad \Gamma_{4,J}^I = \begin{bmatrix} -1 & 0 & 0 & 0 \\ 0 & -1 & 0 & 0 \\ 0 & 0 & -1 & 0 \\ 0 & 0 & 0 & -1 \end{bmatrix}. \quad (82)$$

371 The quantities with tildes are defined as:

$$\begin{aligned} \tilde{\epsilon}^A{}_{BC} &= g_2 \epsilon^A{}_{BC} && \text{with } \tilde{\epsilon}^1{}_{23} = g_2 \quad \text{and } \tilde{\epsilon}^4{}_{BC} = 0, \\ \tilde{\gamma}_{A,J}^I &= \begin{cases} g_2 \gamma_{A,J}^I, & \text{for } A = 1, 2, 3, \\ g_1 \gamma_{A,J}^I, & \text{for } A = 4. \end{cases} \end{aligned} \quad (83)$$

372 The relation between barred and unbarred couplings is:

$$\bar{g}_2 = g_2 \sqrt{g}^{11} = g_2 \sqrt{g}^{22}, \quad (84)$$

$$\bar{g}_Z = \frac{g_2}{c_{\theta_Z}^2} (\bar{c}_W \sqrt{g}^{33} - \bar{s}_W \sqrt{g}^{34}) = \frac{g_1}{s_{\theta_Z}^2} (\bar{s}_W \sqrt{g}^{44} - \bar{c}_W \sqrt{g}^{34}), \quad (85)$$

$$\bar{e} = g_1 (\bar{s}_W \sqrt{g}^{33} + \bar{c}_W \sqrt{g}^{34}) = g_1 (\bar{c}_W \sqrt{g}^{44} + \bar{s}_W \sqrt{g}^{34}). \quad (86)$$

373 The above expressions make use of the barred mixing angles:

$$s_{\theta_Z}^2 = \frac{g_1(\sqrt{g}^{44} \bar{s}_W - \sqrt{g}^{34} \bar{c}_W)}{g_2(\sqrt{g}^{33} \bar{c}_W - \sqrt{g}^{34} \bar{s}_W) + g_1(\sqrt{g}^{44} \bar{s}_W - \sqrt{g}^{34} \bar{c}_W)}, \quad (87)$$

$$\bar{s}_W^2 = \frac{(g_1 \sqrt{g}^{44} - g_2 \sqrt{g}^{34})^2}{g_1^2[(\sqrt{g}^{34})^2 + (\sqrt{g}^{44})^2] + g_2^2[(\sqrt{g}^{33})^2 + (\sqrt{g}^{34})^2] - 2g_1 g_2 \sqrt{g}^{34}(\sqrt{g}^{33} + \sqrt{g}^{44})} \quad (88)$$

374 The barred masses are given by:

$$\bar{M}_W^2 = \frac{\bar{g}_2^2}{4} \sqrt{h_{11}}^{-2} v^2, \quad (89)$$

$$\bar{M}_Z^2 = \frac{\bar{g}_Z^2}{4} \sqrt{h_{33}}^{-2} v^2, \quad (90)$$

$$\bar{M}_A^2 = 0. \quad (91)$$

375 Expanding the elements of the field-space connections of Eqs. 13–17 become complicated
 376 very quickly, supporting the use of the geometric approach. Some examples of elements
 377 of the matrices include:

$$\sqrt{g}^{11} = 1 + c_{HW}^{(6)} v^2 + \frac{1}{2} [c_{HW}^{(8)} + 3(c_{HW}^{(6)})^2] v^4 \quad (92)$$

$$\sqrt{h}^{44} = 1 + \frac{1}{4} [4c_{H\Box}^{(6)} - c_{HD}^{(6)}] v^2 + \frac{1}{32} [3(c_{HD}^{(6)} - c_{H\Box}^{(6)})^2 - 4c_{HD}^{(8)} - 4c_{HD,2}^{(8)}] v^4 + \mathcal{O}\left(\frac{1}{\Lambda^6}\right) \quad (93)$$

378

379 B Relevance of the tadpole to renormalization

380 Here we outline the importance of the tadpole to renormalization. We proceed by outline
 381 the renormalization procedure to arrive at the implications of the tadpole diagram in the
 382 FJ tadpole scheme, we do not employ the BFM here for simplicity. We loosely follow the
 383 notation of [15]. The fields are renormalized as follows:

$$h_0 = \sqrt{Z_h} h_R \quad (94)$$

$$W_0^\pm = \sqrt{Z_W} W_R^\pm \quad (95)$$

$$(96)$$

384 The fourth component of the real scalar field is renormalized as:

$$\phi_4 = v_0 + \hat{h}_0 \rightarrow Z_v v_R + \delta v + \sqrt{Z_h} h_R \quad (97)$$

385 Expanding the scalar potential of Eq. 11 about the tree level vacuum expectation value
 386 and adding the one-loop tadpole contribution we find:

$$t = -2\lambda_R v_R \delta v + T_H \equiv \delta t + T_H \quad (98)$$

387 This defines the relationship between δt and δv , in the main text δt is chosen such that
 388 $t = 0$. This is equivalent to the choice:

$$\delta v = \frac{1}{2\lambda_R v_R^2} T_H = \frac{1}{M_{H,R}^2} T_H \quad (99)$$

389 Employing an on-shell renormalization scheme as in [15] the one loop shifts in masses
 390 of the vector bosons ($V = W, Z$) are given by:

$$\frac{\bar{m}_{V,R}^2}{\bar{m}_V^2} = 1 + 2\frac{\delta v}{v} - \frac{\delta m_V^2}{m_V^2}, \quad (100)$$

391 where δv corresponds to the correction outlined above, and δm_V^2 corresponds to the explicit
 392 contribution from the transverse part of the one-loop two-point functions:

$$\delta m_V^2 = \text{Re}[\Sigma_T^{VV}(M_p^2)]. \quad (101)$$

393 In this way we can see from Eq. 100 that even in the FJ tadpole scheme employed in
 394 this article, the one-loop tadpole is still phenomenologically relevant as it shifts the masses
 395 of the gauge bosons. Further, as the tadpole was found to be gauge-parameter dependent
 396 in Sec 5, we see that the gauge-independence of results such as the shifted masses depend
 397 on the tadpole diagram. In this way we have demonstrated the importance of the tadpole
 398 diagram to the future one-loop geoSMEFT program both phenomenologically and in terms
 399 of gauge invariance of the theory, which is necessary for the consistency of the QFT.

References

- 400
- 401 [1] C. Hays, A. Martin, V. Sanz and J. Setford, *On the impact of dimension-*
402 *eight SMEFT operators on Higgs measurements*, JHEP **02**, 123 (2019),
403 doi:10.1007/JHEP02(2019)123, 1808.00442.
- 404 [2] L. Lehman and A. Martin, *Hilbert Series for Constructing Lagrangians: ex-*
405 *anding the phenomenologist's toolbox*, Phys. Rev. D **91**, 105014 (2015),
406 doi:10.1103/PhysRevD.91.105014, 1503.07537.
- 407 [3] L. Lehman and A. Martin, *Low-derivative operators of the Standard Model*
408 *effective field theory via Hilbert series methods*, JHEP **02**, 081 (2016),
409 doi:10.1007/JHEP02(2016)081, 1510.00372.
- 410 [4] B. Henning, X. Lu, T. Melia and H. Murayama, *2, 84, 30, 993, 560, 15456, 11962,*
411 *261485, ...: Higher dimension operators in the SM EFT*, JHEP **08**, 016 (2017),
412 doi:10.1007/JHEP08(2017)016, [Erratum: JHEP 09, 019 (2019)], 1512.03433.
- 413 [5] R. Boughezal, E. Mereghetti and F. Petriello, *Dilepton production in the SMEFT at*
414 $\mathcal{O}(1/\Lambda^4)$ (2021), 2106.05337.
- 415 [6] T. Corbett, A. Helset, A. Martin and M. Trott, *EWPD in the SMEFT to dimension*
416 *eight* (2021), 2102.02819.
- 417 [7] C. Hartmann and M. Trott, *On one-loop corrections in the standard model*
418 *effective field theory; the $\Gamma(h \rightarrow \gamma\gamma)$ case*, JHEP **07**, 151 (2015),
419 doi:10.1007/JHEP07(2015)151, 1505.02646.
- 420 [8] C. Hartmann and M. Trott, *Higgs Decay to Two Photons at One Loop in the*
421 *Standard Model Effective Field Theory*, Phys. Rev. Lett. **115**(19), 191801 (2015),
422 doi:10.1103/PhysRevLett.115.191801, 1507.03568.
- 423 [9] A. Helset, M. Paraskevas and M. Trott, *Gauge fixing the Standard*
424 *Model Effective Field Theory*, Phys. Rev. Lett. **120**(25), 251801 (2018),
425 doi:10.1103/PhysRevLett.120.251801, 1803.08001.
- 426 [10] A. Helset, A. Martin and M. Trott, *The Geometric Standard Model Effective Field*
427 *Theory*, JHEP **03**, 163 (2020), doi:10.1007/JHEP03(2020)163, 2001.01453.
- 428 [11] C. Hays, A. Helset, A. Martin and M. Trott, *Exact SMEFT formulation and expansion*
429 *to $\mathcal{O}(v^4/\Lambda^4)$* , JHEP **11**, 087 (2020), doi:10.1007/JHEP11(2020)087, 2007.00565.
- 430 [12] T. Corbett, *The Feynman rules for the SMEFT in the background field gauge*, JHEP
431 **03**, 001 (2021), doi:10.1007/JHEP03(2021)001, 2010.15852.
- 432 [13] J. Fleischer and F. Jegerlehner, *Radiative Corrections to Higgs Decays*
433 *in the Extended Weinberg-Salam Model*, Phys. Rev. D **23**, 2001 (1981),
434 doi:10.1103/PhysRevD.23.2001.
- 435 [14] A. Denner, G. Weiglein and S. Dittmaier, *Application of the background field method*
436 *to the electroweak standard model*, Nucl. Phys. B **440**, 95 (1995), doi:10.1016/0550-
437 3213(95)00037-S, hep-ph/9410338.
- 438 [15] T. Corbett, A. Martin and M. Trott, *Consistent higher order $\sigma(\mathcal{G}\mathcal{G} \rightarrow h)$, $\Gamma(h \rightarrow \mathcal{G}\mathcal{G})$*
439 *and $\Gamma(h \rightarrow \gamma\gamma)$ in geoSMEFT* (2021), 2107.07470.

- 440 [16] T. Corbett and M. Trott, *One loop verification of SMEFT Ward Identities* (2020),
441 2010.08451.
- 442 [17] T. Corbett, A. Helset and M. Trott, *Ward Identities for the Stan-*
443 *dard Model Effective Field Theory*, Phys. Rev. D **101**(1), 013005 (2020),
444 doi:10.1103/PhysRevD.101.013005, 1909.08470.
- 445 [18] W. Dekens and P. Stoffer, *Low-energy effective field theory below the electroweak*
446 *scale: matching at one loop*, JHEP **10**, 197 (2019), doi:10.1007/JHEP10(2019)197,
447 1908.05295.
- 448 [19] G. Buchalla, A. Celis, C. Krause and J.-N. Toelstede, *Master Formula for One-Loop*
449 *Renormalization of Bosonic SMEFT Operators* (2019), 1904.07840.